Published in final edited form as:
Vascul Pharmacol. 2013 January ; 58(1-2): 87–97. doi:10.1016/j.vph.2012.08.003.

Nicotinic Acetylcholine Receptor Mediates Nicotine-Induced Actin Cytoskeletal Remodeling and Extracellular Matrix Degradation by Vascular Smooth Muscle Cells

Zhizhan Gu[a], **Vera Fonseca**[b], and **Chi-Ming Hai**[b]

[a]Division of Rheumatology, Immunology and Allergy, Department of Medicine, Brigham and Women's Hospital, Harvard Medical School, Boston, MA 02115

[b]Department of Molecular Pharmacology, Physiology & Biotechnology, Brown University, Providence, RI 02912, USA

Abstract

Cigarette smoking is a significant risk factor for atherosclerosis, which involves the invasion of vascular smooth muscle cells (VSMCs) from the media to intima. A hallmark of many invasive cells is actin cytoskeletal remodeling in the form of podosomes, accompanied by extracellular matrix (ECM) degradation. A7r5 VSMCs form podosomes in response to PKC activation. In this study, we found that cigarette smoke extract, nicotine, and the cholinergic agonist, carbachol, were similarly effective in inducing the formation of podosome rosettes in A7r5 VSMCs. α-Bungarotoxin and atropine experiments confirmed the involvement of nicotinic acetylcholine receptors (nAChRs). Western blotting and immunofluorescence experiments revealed the aggregation of nAChRs at podosome rosettes. Cycloheximide experiments and media exchange experiments suggested that autocrine factor(s) and intracellular phenotypic modulation are putative mechanisms. In situ zymography experiments indicated that, in response to PKC activation, nicotine-treated cells degraded ECM near podosome rosettes, and possibly endocytose ECM fragments to intracellular compartments. Invasion assay of human aortic smooth muscle cells indicated that nicotine and PKC activation individually and synergistically enhanced cell invasion through ECM. Results from this study suggest that nicotine enhances the ability of VSMCs to degrade and invade ECM. nAChR activation, actin cytoskeletal remodeling and phenotypic modulation are possible mechanisms.

Keywords

Cigarette smoking; cytoskeletal remodeling; cell invasion; nicotine; vascular smooth muscle

1. Introduction

Cigarette smoking is a significant risk factor for atherosclerosis, which involves the invasion of vascular smooth muscle cells from the media to intima (Balakumar and Kaur, 2009;

Correspondence: Chi-Ming Hai, PhD Brown University, Box G-B3 171 Meeting Street Providence, RI 02912 USA Tel. 1-401-863-3288 Fax. 1-401-863-1440 chi-ming_hai@brown.edu.

Doran et al., 2008; Erhardt, 2009; Newby, 2005). Nicotine and nicotinic acetylcholine receptors are known to mediate smoking addition, and their roles in stimulating angiogenesis have been studied extensively, as reviewed by Cooke and Ghebremariam (2008) and Egleton et al. (2009). For example, using mouse models of lung cancer and atherosclerosis, Heeshen et al. (2001) were the first to show that nicotine stimulates angiogenesis and promotes tumor growth and atherosclerosis by activating nicotinic acetylcholine receptors in endothelial cells. Other studies together showed that all components for synthesizing and degrading acetylcholine are present in endothelial cells, suggesting that endogenous acetylcholine functions as autocrine and/or paracrine in endothelial cells. Ng et al. (2007) established the physiological significance of nicotinic acetylcholine receptors in endothelial cell migration by showing that activation of nicotinic acetylcholine receptor is required for growth factor-induced endothelial cell migration. Thus, there is consensus among endothelial biologists that nicotine stimulates angiogenesis by activating nicotinic acetylcholine receptors in endothelial cells. In contrast, the effect of nicotine and function of nicotinic acetylcholine receptor in vascular smooth muscle invasion are not fully understood.

A hallmark of many invasive cells is actin cytoskeletal remodeling in the form of podosomes, accompanied by extracellular matrix degradation (Gimona and Buccione, 2006; Linder, 2006). We and others have reported the formation of podosomes by A7r5 vascular smooth muscle cells in response to PKC activation (Burgstaller and Gimona, 2005; Dorfleutner et al., 2008; Eves et al., 2006; Gu et al., 2007; Hai et al., 2002; Wang et al., 2010). In this study, we tested the hypothesis that nicotinic acetylcholine receptor mediates cigarette smoke extract and nicotine-induced actin cytoskeletal remodeling and extracellular matrix degradation by A7r5 vascular smooth muscle cells in response to PKC activation. In addition, we investigated the individual and interactive effects of nicotine and PKC activation on invasion of human aortic smooth muscle cells.

We identified nicotinic acetylcholine receptors and podosome-associated proteins in A7r5 cells by Western blotting and immunofluorescence microscopy. We differentiated the functions of nicotinic and muscarinic acetylcholine receptors in mediating nicotine-induced actin cytoskeletal remodeling using the nicotinic and muscarinic acetylcholine receptor antagonists, α-bungarotoxin and atropine, respectively. We investigated the involvement of phenotypic modulation in nicotine-induced actin cytoskeletal remodeling by performing cycloheximide and media exchange experiments. We studied nicotine-induced extracellular matrix degradation by A7r5 cells by performing in situ zymography experiments using cross-linked Alexa Fluor 488-conjugated gelatin and DQ-gelatin. Finally, we investigated the individual and interactive effects of nicotine and PKC activation on invasion of human aortic smooth muscle cells using matrigel-coated transwell assay. Results from this study suggest that long-term exposure to nicotine enhances the ability of VSMCs to degrade and invade ECM. Nicotinic acetylcholine receptor activation, actin cytoskeletal remodeling and phenotypic modulation are possible mechanisms.

2. Materials and methods

2.1. Cell Culture

The procedure was the same as described previously (Gu et al., 2007). A7r5 rat vascular smooth muscle cells were purchased from ATCC (Manasas, VA), and grown in low-glucose (1000 mg/ml) DMEM without phenol red, supplemented with 10% fetal bovine serum, GlutaMAX™-I Supplement, and penicillin/streptomycin at 37°C and 5% CO2. Human aortic smooth muscle cells were purchased from Invitrogen (Grand Island, NY) and cultured in medium 231, supplemented with smooth muscle differentiation supplement, according to the vendor's instructions. All cell culture reagents were purchased from Invitrogen (Grand

Island, NY). Podosome formation in cultured A7r5 cells was induced by 1 μM phorbol-12,13-dibutyrate (PDBu; Sigma) in serum-free medium.

2.2. Cigarette Smoke Extract Experiments

The procedure was similar to that described by Su et al. (1998). Briefly, cigarette smoke extract was prepared by bubbling cigarette smoke through 30 ml sterile phosphate-buffered saline (PBS) of the following composition: 138 mM NaCl, 26 mM KCl, 84 mM Na_2HPO_4, pH 7.4 (37°C) using a vacuum pump. Each cigarette was "smoked" for 5 min, and six cigarettes were used per 30 ml PBS to generate a cigarette smoke extract. The [nicotine] in this cigarette smoke extract should be approximately 15 μM (Lee et al., 2001). Since the average plasma [nicotine] in chronic smokers was approximately 1 μM (Moreyra et al., 1992), we studied the effect of 5% cigarette smoke extract on A7r5 cells.

2.3. Confocal Immunofluorescence Microscopy

The procedure was the same as described previously (Gu et al., 2007). For immunofluorescence microscopy studies, cells cultured on 15-mm glass coverslips were washed three times in PBS, fixed in 4% paraformaldehyde (Electron Microscopy Sciences, Hatfield, PA) in PBS for 15 min, and extracted with 0.3% Triton X-100 in PBS for 10 min. Coverslips containing triton-extracted cells were labeled with primary antibodies for 1 hr, washed three times in PBS, incubated with secondary antibodies, washed three times in PBS, and then mounted on glass slides with FluorSave™ Reagent (Calbiochem, San Diego, CA). Immunofluorecence images were captured using a Leica TCS SP2 AOBS confocal microscope equipped with a 63× 1.4 Plan Aprochromatic oil-immersion objective and a digital camera controlled by Leica Confocal Software package (version 2.5; Leica Microsystems, Exton, PA).

2.4. SDS-Polyacrylamide Gel Electrophoresis (SDS-PAGE) and Western Blot Analysis

The procedure was the same as described previously (Gu et al., 2007). For SDS-PAGE, A7r5 cells were lysed and scraped with an ice-cold cell lysis buffer of the following composition: 1% Triton X-100, 50 mM HEPES, 150 mM NaCl, 5 mM EDTA, 5 mM EGTA, 20 mM NaF, 20 mM sodium pyrophosphate, 1 mM PMSF, 1 mM Na_2VO4; pH 7.4. DC protein assays (Bio-Rad Laboratories, Hercules, CA) were performed on cell lysate samples. Equal amount of protein from each sample was run on each lane of 7.5% SDS-PAGE gels. After gel electrophoresis, proteins were transferred to nitrocellulose membranes for Western blot analysis. Proteins on the membranes were labeled with primary antibodies overnight at 4°C, then labeled by peroxidase-conjugated secondary antibodies, and visualized by Enhanced Chemiluminenescence detection reagents (Amersham Biosciences, Piscataway, NJ).

2.5. In Situ Zymography of Extracellular Matrix Degradation

We studied nicotine-induced extracellular matrix degradation by A7r5 cells by performing in situ zymography experiments using two different substrates - cross-linked Alexa Fluor 488-conjugated gelatin and DQ-gelatin. The cross-linked Alexa Fluor 488-conjugated gelatin method was similar to that described by Bowden et al. (2001). Briefly, glass coverslips were covered by 0.5 mg/ml crosslinker SulfoSANPHA (G-Biosciences) in PBS, followed by ultraviolet irradiation for 10 min to cross-link one end of the SulfoSANPHA molecule to glass. After ultraviolet irradiation, coverslips were washed three times with PBS, and then incubated with 0.1 mg/ml Alexa Fluor 488-conjugated gelatin (Invitrogen) for 4 hrs to cross-link Alexa Fluor 488-conjugated gelatin to the free end of SulfoSANPHA . A7r5 cells were seeded onto cross-linked Alexa Fluor 488-conjugated gelatin-coated coverslips in 10% serum-containing media for 2 hrs to allow cell attachment. The serum-

containing media was then replaced with serum-free media to minimize the release of metalloproteinase by cells during overnight incubation. Cells were cultured overnight in serum-free media with or without 2 μM nicotine, depending on the experiment, and then stimulated by 1 μM PDBu for 1 hr.

The DQ-gelatin method was similar to that described by Busco et al. (2010) and Cortesi et al. (1998). Briefly, a PBS solution containing 5% bovine skin gelatin (Sigma-Aldrich; St. Louis, MO) and 2.5% sucrose was prepared by heating the solution to 40°C. DQ-gelatin (Invitrogen) was then added to the solution at a final concentration of 30 μg/ml. Glass coverslips were coated with the sucrose-gelatin/DQ-gelatin mix and stored in the refrigerator. DQ-gelatin-coated coverslips were equilibrated in a cell culture incubator for 1 hr, incubated in culture media for 1 hr, plated with A7r5 cells, and then incubated overnight before treatment with nicotine and/or PDBu. At the end of an experiment, A7r5 cells were fixed with 4% paraformaldehyde, labeled with the nuclear stain DAPI, and then imaged using a Nikon Diaphot 300 fluorescence microscope equipped with a 40x Plan Aprochromatic oil-immersion objective and a digital camera (Zeiss Axiocam) controlled by the Zeiss Axiovision software.

2.6 Transwell Invasion Assay

The method for studying invasion of human aortic smooth muscle cells through extracellular matrix using a matrigel-coated transwell system (BD Biosciences, San Jose, CA) was similar to that described by Maqbool et al. (2012). Briefly, human aortic smooth muscle cells (5×10^4; Invitrogen, Grand Island, NY) were loaded onto the matrigel-coated membrane in the upper chamber of the transwell system, and allowed to invade through the matrigel to the bottom side of the membrane for 24 hrs. The upper chamber contained serum-free 231 medium (Invitrogen, Grand Island, NY), whereas the lower chamber contained the 231 medium and 0.1% smooth muscle differentiation supplement (SMDS; Invitrogen, Grand Island, NY). To investigate the effects of PDBu and nicotine on cell invasion, we added PDBu (2 μM) and/or nicotine (2 μM) to the top or bottom chambers, depending on the experiment. Three transwell experiments were repeated for all experimental groups.

After 24 hr incubation, cells on the top side of the membrane were removed using a cotton-tipped applicator, whereas cells invaded through matrigel to the bottom side of the membrane were fixed by 4% formaldehyde, and then labeled with DRAQ5 (Cell Signaling, Danvers, MA) and Alexa Fluor 546-conjugated phalloidin (Invitrogen, Grand Island, NY). The membrane was then excised for fluorescence microscopy using a 20x objective. Fluorescence from DRAQ5-labeled nuclei appeared as blue, whereas Alexa Fluor 546-conjugated phalloidin-labeled filamentous actin appeared as red. For each membrane, the number of cells in the 20x microscopic field was counted based on DRAQ5-labeled nuclei. Cell counts from three repeat experiments were averaged to calculate the mean and standard deviation. Student's t-test was used for the comparison of two means ($p < 0.05$ considered significant). In addition, two-way ANOVA was performed to analyze individual and interactive effects of PDBu and nicotine on cell invasion ($p < 0.05$).

2.7 Antibodies

PKC-α polyclonal and MMP-2 monoclonal antibodies were purchased from Santa Cruz Biotechnology (Santa Cruz, CA). Anti-vinculin monoclonal antibodies and peroxidase-conjugated secondary antibodies were purchased from Sigma-Aldrich (St. Louis, MO). Alexa Fluor 488 and Alexa Fluor 568-conjugated secondary antibodies and phalloidin were purchased from Molecular Probes (Eugene, OR). Anti-α7-nicotinic acetylcholine receptor polyclonal antibody, Alexa Fluor 647-conjugated bungarotoxin, unconjugated bungarotoxin,

and protein sample from C57 mouse brain were generous gifts from Dr. Edward Hawrot's laboratory at Brown University.

3. Results

3.1. Cigarette Smoke Extract and Nicotine-Induced Cytoskeletal Remodeling in A7r5 Cells in Response to PKC Activation

As shown in Fig. 1A, untreated, unstimulated (control) A7r5 cells formed actin stress fibers and vinculin-containing focal adhesions, with localization of PKC-α and MMP-2 in the perinuclear area. As shown in Fig. 1B, in response to PKC activation by PDBu, untreated A7r5 cells formed podosomes – peripheral dot-like structures having a filamentous actin core surrounded by vinculin, PKC-α, and MMP-2. In contrast, as shown in Fig. 1C, cigarette smoke extract-treated A7r5 cells formed circular cytoskeletal structures localized by filamentous actin, vinculin, PKC-α, and MMP-2, which resembled podosome rosettes in endothelial cells and fibroblasts (Linder, 2006; Varon et al., 2006). We found that 6 hr was the minimum incubation time necessary for cigarette smoke extract -induced formation of podosome rosettes (data not shown). As shown in Fig. 1D, treating A7r5 cells with nicotine was sufficient to induce the formation of podosome rosettes in A7r5 cells in response to PKC activation by PDBu. However, in the absence of PKC activation, nicotine treatment alone had no apparent effect on the organization of actin stress fibers and focal adhesions in unstimulated (control) A7r5 cells (Fig. 2C-a).

3.2. Nicotinic Acetylcholine Receptor Mediates Nicotine-Induced Actin Cytoskeletal Remodeling in A7r5 Cells

As shown in Fig. 2A, Western blot analysis confirmed the expression of α7-nicotinic acetylcholine receptors in A7r5 cells. As shown in Fig. 2B, for untreated cells (control), α-7 nicotinic acetylcholine receptors were localized in the perinuclear area in unstimulated cells and became localized at the podosomes in PDBu-stimulated cells. As shown in Fig. 2C, for nicotine-treated cells, nicotinic acetylcholine receptors were localized in the perinuclear area in unstimulated cells and became localized at the podosome rosettes in PDBu-stimulated cells. Carbachol is a stable analog of acetylcholine. As shown in Fig. 2D, carbachol-treated cells were similar to nicotine-treated cells in forming podosome rosettes in response to PDBu stimulation. Furthermore, as shown in Fig. 2D, for carbachol-treated cells, nicotinic acetylcholine receptors were localized in the perinuclear area in unstimulated cells and became localized at the podosome rosettes in PDBu-stimulated cells.

To further determine the involvement of nicotinic acetylcholine receptors in nicotine-induced cytoskeletal remodeling, we treated A7r5 cells with the nicotinic acetylcholine receptor antagonist α-bungarotoxin (Moise et al., 2002). As shown in Fig. 3, α-bungarotoxin had no apparent effect on the formation of podosomes in untreated cells in response to PDBu stimulation (Fig. 3A), but inhibited the formation of podosome rosettes in nicotine-treated cells in response to PDBu stimulation (Fig. 3B). In the presence of α-bungarotoxin, nicotine-treated cells formed podosomes in response to PDBu stimulation (Fig. 3B).

The relatively long incubation time (6 hr) necessary for nicotine-induced actin cytoskeletal remodeling suggested nicotine-induced phenotypic modulation in A7r5 cells. To determine the necessity of protein synthesis for nicotine-induced actin cytoskeletal remodeling, we treated A7r5 cells with the protein synthesis inhibitor, cycloheximide. As shown in Fig. 3, cycloheximide had no apparent effect on the formation of podosomes in untreated cells in response to PDBu stimulation (Fig. 3C), but inhibited the formation of podosome rosettes in nicotine-treated cells in response to PDBu stimulation (Fig. 3D). In the presence of

cycloheximide, nicotine-treated cells formed podosomes in response to PDBu stimulation (Fig. 3D).

To further differentiate the functions of nicotinic and muscarinic acetylcholine receptors in inducing cytoskeletal remodeling in A7r5 cells, we compared the effects of the nicotinic and muscarinic acetylcholine receptor antagonists, α-bungarotoxin and atropine, respectively, on carbachol-induced actin cytoskeletal remodeling. As shown in Fig. 4, carbachol treatment alone had no apparent effect on the organization of actin stress fibers and focal adhesions in unstimulated cells (Fig. 4A), whereas carbachol-treated cells formed podosome rosettes in response to PDBu stimulation (Fig. 4B). As shown in Fig. 4C, the nicotinic acetylcholine receptor antagonist, α-bungarotoxin, inhibited the ability of carbachol to induce the formation of podosome rosettes in A7r5 cells in response to PDBu stimulation. In the presence of α-bungarotoxin, carbachol-treated cells formed podosomes in response to PDBu stimulation (Fig. 4C). In contrast, the muscarinic acetylcholine receptor antagonist, atropine, did not inhibit the ability of carbachol to induce the formation of podosome rosettes in A7r5 cells (Fig. 4D).

3.3. Autocrine Release and Intracellular Phenotypic Modulation as Putative Mechanisms in Nicotine-Induced Actin Cytoskeletal Remodeling in A7r5 Cells

As shown previously in Figs. 3C and 3D, the cycloheximide experiments suggested that protein synthesis is necessary for nicotine-induced actin cytoskeletal remodeling in A7r5 cells. In principle, nicotine may stimulate A7r5 cells to synthesize and release autocrine factor(s), which then acts on A7r5 cells to induce actin cytoskeletal remodeling. Alternatively, nicotine may stimulate intracellular phenotypic modulation in A7r5 cells to induce actin cytoskeletal remodeling. These two possibilities are not mutually exclusive. To determine the involvement of autocrine factor(s), we investigated whether conditioned media collected from culture of nicotine-treated cells could induce the formation of podosome rosettes in untreated cells in response to PDBu stimulation. As shown in Fig. 5A, in the presence of conditioned media collected from culture of nicotine-treated A7r5 cells, untreated A7r5 cells responded to PDBu stimulation with the formation of filamentous actin dots and patches, most of which were *colocalized* with vinculin. The peripheral filamentous actin dots resembled podosomes in untreated cells (Fig. 1B), whereas the filamentous actin patches resembled incomplete segments of podosome rosettes in nicotine-treated cells (Fig. 1D). To determine the involvement of intracellular phenotypic modulation, we investigated whether nicotine-treated A7r5 cells placed in fresh media would form podosome rosettes in response to PDBu stimulation. As shown in Fig. 5B, nicotine-treated cells placed in fresh media responded to PDBu stimulation with the formation of filamentous actin patches, most of which were *colocalized* with vinculin. This pattern of actin cytoskeletal remodeling was distinct from podosomes in untreated cells (Fig. 1B) and also distinct from podosome rosettes in nicotine-treated cells (Fig. 1D).

3.4. In Situ Zymography of Extracellular Matrix Degradation

To determine the effect of nicotine on the ability of A7r5 vascular smooth muscle cells to degrade extracellular matrix, we performed in situ zymography experiments using two different substrates - cross-linked Alexa Fluor 488-conjugated gelatin and DQ-gelatin. Degradation of cross-linked Alexa Fluor 488-conjugated gelatin results in the loss of fluorescence and the appearance of dark areas under fluorescence microscopy. In contrast, DQ-gelatin is gelatin heavily labeled with FITC, such that the FITC fluorescence becomes quenched. Enzymatic degradation of DQ-gelatin releases fluorescent peptide fragments, which can be imaged using a fluorescence microscope. Furthermore, in situ zymography using DQ-gelatin allows imaging of cellular processing of fluorescent peptide fragments after DQ-gelatin degradation. Thus, the cross-linked Alexa Fluor 488-conjugated gelatin

experiments provide information on localized extracellular matrix degradation, whereas the DQ-gelatin experiments provide information on extracellular matrix degradation and cellular processing of degraded extracellular matrix.

As shown in Fig. 6 (top row, “No stimulation”), after overnight plating on cross-linked Alexa Fluor 488-conjugated gelatin, an unstimulated, untreated cell exhibited some basal activity of extracellular matrix degradation, as indicated by the dark area within the boundaries of F-actin stress fibers. Similarly, a nicotine-treated, unstimulated cell also exhibited some basal activity of extracellular matrix degradation, as indicated by the dark area within the boundaries of F-actin stress fibers (Fig. 6, second row, “Nicotine”). However, in response to PKC activation, untreated cells degraded extracellular matrix in the proximity of podosomes (Fig. 6, third row, “PDBu”), whereas nicotine-treated cells degraded extracellular matrix in the proximity of podosome rosettes (Fig. 6, bottom row, “Nicotine + PDBu”). Furthermore, the intensity of extracellular matrix degradation, as indicated by the degree of darkness, appeared to be greater near podosome rosettes than podosomes (Fig. 6, bottom two rows).

As shown in Fig. 7A (left panel), after overnight plating on DQ-gelatin, control cells exhibited a fibrous network of fluorescence in the cell periphery, indicating some basal activity of extracellular matrix degradation. Similarly, nicotine-treated cells, after overnight plating on DQ-However, PDBu stimulation of control cells plated on DQ-gelatin resulted in the circumferential distribution of fluorescence dots of DQ-gelatin fragments (Fig. 7A, right panel), whereas PDBu stimulation of nicotine-treated cells resulted in the accumulation of patches of DQ-gelatin fragments at the perinuclear region (Fig. 2B, right panel).

3.5. Nicotine and PDBu-Induced Invasion of Human Aortic Smooth Muscle Cells Through Extracellular Matrix

To investigate the effects of PKC activation and nicotine on invasiveness of primary vascular smooth muscle cells, we studied the invasion of human aortic smooth muscle cells using matrigel-coated transwell assay. To investigate the effects of PDBu and nicotine on cell invasion, we added PDBu (2 μM) and/or nicotine (2 μM) to the top or bottom chambers in the following four groups of experiments: (A) No Stimulation: neither nicotine nor PDBu was added to the top or bottom chamber; (B) PDBu: 2 μM PDBu in the bottom chamber only; (C) Nicotine: 2 μM nicotine in both top and bottom chambers; and (D) Nicotine + PDBu: 2 μM nicotine in top chamber; 2 μM nicotine and 2 μM PDBu in the bottom chamber. Prior to invasion assay, cells in groups A and B were cultured in 231 medium with 1% SMDS for 16 hr, whereas cells in groups C and D were cultured in 231 medium with 1% SMDS and 2 μM nicotine. As shown in Fig. 8 (panels A-C), PKC activation by PDBu and nicotine individually increased the number of cells invading through matrigel to reach the bottom side of the membrane by 280% and 150%, respectively . As shown in Fig. 8 (panel D), nicotine and PDBu together increased the number of cells invading through matrigel by 720%, which was larger than the sum of increases induced by nicotine and PDBu individually. Two-way ANOVA indicated significant individual and interactive effects of PDBu and nicotine on cell invasion ($p < 0.05$).

4. Discussion

Cigarette smoking is a significant risk factor for atherosclerosis, a vascular disease characterized by the invasion of vascular smooth muscle cells from the media to intima. A hallmark of many invasive cells is actin cytoskeletal remodeling in the form of podosomes, accompanied by extracellular matrix degradation (Gimona and Buccione, 2006; Linder, 2006). We and others have reported the formation of podosomes in A7r5 vascular smooth muscle cells in response to PKC activation (Burgstaller and Gimona, 2005; Dorfleutner et

al., 2008; Eves et al., 2006; Gu et al., 2007; Hai et al., 2002; Wang et al., 2010). As shown in Fig. 1A, control cells formed actin stress fibers anchored at vinculin-containing focal adhesions. Activation of PKC by PDBu induced the disassembly of actin stress fibers to form dot-like filamentous actin-rich podosomes in the cell periphery (Fig. 1B). As described previously (Gu et al., 2007; Hai et al., 2002), podosomes are actin cytoskeletal columns extending from the cell base towards the cell surface, consisting of a filamentous actin core, surrounded by a ring of actin-binding proteins such as α-actinin, caldesmon, and vinculin. Several laboratories, including ours, have shown that the conventional PKC isoform, PKC-α, mediates PDBu-induced formation of podosomes in vascular smooth muscle cells. In this study, we found that cigarette smoke extract, nicotine, and carbachol induced the formation of circular actin cytoskeletal structures in A7r5 vascular smooth muscle cells in response to PKC activation (Figs. 1 and 2). These circular cytoskeletal structures are enriched in filamentous actin, vinculin, PKC-α and MMP-2 – proteins that are also localized at the podosomes in A7r5 vascular smooth muscle cells (Gu et al., 2007; Hai et al., 2002). These circular cytoskeletal structures are similar to podosome rosettes observed in endothelial cells and fibroblasts in having a circular structure and requiring protein synthesis for formation (Varon et al., 2006). Therefore, we tentatively consider these circular cytoskeletal structures as podosome rosettes in A7r5 vascular smooth muscle cells. To our knowledge, this is the first report of podosome rosette formation in vascular smooth muscle cells. Podosomes and podosome rosettes are invasive/adhesive cellular structures for extracellular matrix degradation (Linder, 2006). Therefore, the finding that nicotine is as effective as cigarette smoke extract in stimulating the formation of podosome rosettes in vascular smooth muscle cells suggests that replacing cigarette smoking by nicotine treatment may have limited beneficial effects on atherosclerosis, providing support to the emerging recognition that nicotine is a key player in atherosclerosis (Balakumar and Kaur, 2009).

The finding that the cholinergic receptor agonist, carbachol, was as effective as nicotine in inducing the formation of podosome rosettes in A7r5 vascular smooth muscle cells (Fig. 4) indicated that acetylcholine receptor mediates nicotine-induced formation of podosome rosettes in A7r5 vascular smooth muscle cells. Results from the α-bungarotoxin and atropine experiments confirmed specifically that nicotinic acetylcholine receptor mediates nicotine-induced formation of podosome rosettes in A7r5 vascular smooth muscle cells (Figs. 2-4). Furthermore, Western blotting and immunofluorescence experiments revealed the aggregation of nicotinic acetylcholine receptors at the podosomes and podosome rosettes in A7r5 vascular smooth muscle cells (Fig. 2). Vascular smooth muscle cells are known to express nicotinic acetylcholine receptors (Bruggmann et al., 2002, 2003); however, to our knowledge, this is the first demonstration of the localization of nicotinic acetylcholine receptors at podosomes and podosome rosettes and the first report of nicotinic acetylcholine receptor-mediated formation of podosome rosettes in vascular smooth muscle cells.

Synthesis of new protein factor(s) appears to be necessary for nicotine-induced formation of podosome rosettes in A7r5 smooth muscle, as suggested by the cycloheximide experiments (Fig. 3D). Vascular smooth muscle cells are capable of synthesizing and releasing autocrine factors (Carty et al., 1996; Cucina et al., 2000). Results from the conditioned media experiments suggest that autocrine factor(s) could be involved in nicotine-induced cytoskeletal remodeling in A7r5 vascular smooth muscle cells (Fig. 5A). In addition, the finding that nicotine-treated cells placed in fresh media formed vinculin-containing actin cytoskeletal patches instead of podosomes (Fig. 5B) suggested that nicotine also induces intracellular phenotypic modulation in A7r5 vascular smooth muscle cells. Altogether, results from these experiments suggest that synthesis of new protein(s) in the form of autocrine factor(s) and intracellular phenotypic modulation are both involved in nicotine-induced formation of podosome rosettes in A7r5 cells.

Degradation of extracellular matrix is a necessary step for tissue invasion of vascular smooth muscle cells from the media to intima in atherosclerosis. Results from in situ zymography experiments using cross-linked Alexa Fluor 488-conjugated gelatin indicated that, in the absence of PKC activation, untreated and nicotine-treated A7r5 cells were similar in exhibiting some basal activity of extracellular matrix degradation (Figs. 6). However, untreated and nicotine-treated cells responded to PKC activation with different patterns of extracellular matrix degradation. In response to PKC activation, untreated cells degraded extracellular matrix in the proximity of podosomes, whereas nicotine-treated cells degraded extracellular matrix in the proximity of podosome rosettes (Fig. 6). Furthermore, the intensity of extracellular matrix degradation appeared to be greater near podosome rosettes than podosomes.

Results from in situ zymography experiments using DQ-gelatin (Fig. 7) were consistent with those using cross-linked Alexa Fluor 488-conjugated gelatin (Fig. 6) in showing extracellular matrix degradation near podosomes. In addition, results from the DQ-gelatin experiments revealed remodeling of DQ-gelatin fragments after degradation. In the absence of PKC activation, both untreated and nicotine-treated cells exhibited some basal activity of extracellular matrix degradation, as reflected by the fluorescence of DQ-gelatin fragments, and, in addition, exhibited organization of DQ-gelatin fragments in the form of a fibrous network (Fig. 7, left panels). In response to PKC activation, untreated cells concentrated DQ-gelatin fragments at circumferential spots, resembling the localization of podosomes (Fig. 7). In contrast, nicotine-treated cells concentrated patches of DQ-gelatin fragments at the perinuclear region (Fig. 7). A possible explanation for this novel observation is that nicotine-treated A7r5 vascular smooth muscle cells may be similar to fibroblasts in having the ability to phagocytose extracellular matrix fragments and translocate them to intracellular compartments (Everts et al., 1994; Madsen et al., 2007). To our knowledge, this is the first report of using the DQ-gelatin method for demonstrating extracellular matrix remodeling by vascular smooth muscle cells during podosome formation. Future studies are needed to elucidate the underlying mechanisms.

To investigate the effects of PKC activation and nicotine on invasiveness of primary vascular smooth muscle cells, we studied the invasion of human aortic smooth muscle cells using matrigel-coated transwell assay (Fig. 8). We found that both nicotine and PKC activation individually increased cell invasion through matrigel, but the combined effects of PKC activation and nicotine appeared to be greater than the sum of individual PKC and nicotine effects on cell invasion. Consistently, two-way ANOVA of the cell count data indicated significant individual and synergistic effects of PKC activation and nicotine on the invasion of human aortic smooth muscle cells through matrigel.

In summary, results from this study suggest that long-term exposure to nicotine enhances the ability of vascular smooth muscle cells to degrade and invade extracellular matrix. Nicotinic acetylcholine receptor activation, actin cytoskeletal remodeling and phenotypic modulation are possible mechanisms. A potential implication of this study is that replacing cigarette smoking by nicotine may have limited beneficial effects on atherosclerosis. Understanding the molecular mechanisms linking nicotine acetylcholine receptor activation and vascular smooth muscle invasiveness may lead to new therapeutic approaches for invasive vascular diseases such as atherosclerosis.

Acknowledgments

This study was supported by NIH grant R56-HL-52714. We thank Dr. Eward Hawrot for providing the α7-nicotinic acetylcholine receptor polyclonal antibody, bungarotoxin, Alexa Fluor 647-conjugated bungarotoxin, and α7-nicotinic acetylcholine receptor protein sample from C57 mouse brain for this study. We thank Dr. Stephen J. Reshkin for providing the protocol for DQ-gelatin experiments.

References

Balakumar P, Kaur J. Is nicotine a key player or spectator in the induction and progression of cardiovascular disorders? Pharmacol. Res. 2009; 60:361–368. [PubMed: 19559087]

Bowden ET, Coopman PJ, Mueller SC. Invadopodia: unique methods for measurement of extracellular matrix degradation in vitro. Methods Cell. Biol. 2001; 63:613–627. [PubMed: 11060862]

Bruggmann D, Lips KS, Pfeil U, Haberberger RV, Kummer W. Multiple nicotinic acetylcholine receptor alpha-subunits are expressed in the arterial system of the rat. Histochem Cell. Biol. 2002; 118:441–447. [PubMed: 12483309]

Bruggmann D, Lips KS, Pfeil U, Haberberger RV, Kummer W. Rat arteries contain multiple nicotinic acetylcholine receptor α-subunits. Life Sc. 2003; 72:2095–2099. [PubMed: 12628463]

Burgstaller G, Gimona M. Podosome-mediated matrix resorption and cell motility in vascular smooth muscle cells. Am. J. Physiol. Heart Circ. Physiol. 2005; 288:H3001–H3005. [PubMed: 15695563]

Busco G, Cardone RA, Greco MR, Bellizzi A, Colella M, Antelmi E, Mancini MT, Dell'Aquila ME, Casavola V, Paradiso A, Reshkin SJ. NHE1 promotes invadopodial ECM proteolysis through acidification of the peri-invadopodial space. FASEB J. 2010; 24:3903–3915. [PubMed: 20547664]

Carty CS, Soloway PD, Kayastha S, Bauer J, Marsan B, Ricotta JJ, Dryjski M. Nicotine and cotinine stimulate secretion of basic fibroblast growth factor and affect expression of matrix metalloproteinases in cultured human smooth muscle cells. J. Vasc. Surg. 1996; 24:927–935. [PubMed: 8976346]

Catanzaro DF, Zhou Y, Chen R, Yu F, Catanzaro SE, De Lorenzo MS, Subbaramaiah K, Zhou XK, Pratico D, Dannenberg AJ, Weksler BB. Potentially reduced exposure cigarettes accelerate atherosclerosis: evidence for the role of nicotine. Cardiovasc. Toxicol. 2007; 7:192–201. [PubMed: 17901562]

Cooke JP, Ghebremariam YT. Endothelial nicotinic acetylcholine receptors and angiogenesis. Trends Cardiovasc. Med. 2008; 18:247–253. [PubMed: 19232953]

Cortesi R, Nastruzzi C, Davis SS. Sugar cross-linked gelatin for controlled release: microspheres and disks. Biomaterials. 1998; 19:1641–1649. [PubMed: 9839999]

Cucina A, Sapienza P, Corvino V, Borrelli V, Randone B, D'Angelo LS, Cavallaro A. Nicotine induces platelet-derived growth factor release and cytoskeletal alteration in aortic smooth muscle cells. Surgery. 2000; 127:72–78. [PubMed: 10660761]

Cucina A, Fuso A, Coluccia P, Cavallaro A. Nicotine inhibits apoptosis and stimulates proliferation in aortic smooth muscle cells through a functional nicotinic acetylchoine receptor. J. Surg. Res. 2008; 150:227–235. [PubMed: 18295799]

Doran AC, Meller N, McNamara CA. Role of smooth muscle cells in the initiation and early progression of atherosclerosis. Arterioscler. Thromb. Vasc. Biol. 2008; 28:812–819. [PubMed: 18276911]

Dorfleutner A, Cho Y, Vincent D, Cunnick J, Lin H, Weed SA, Stehlik C, Flynn DC. Phosphorylation of AFAP-110 affects podosome lifespan in A7r5 cells. J. Cell Sci. 2008; 121:2394–2405. [PubMed: 18577577]

Egelton RD, Brown KC, Dasgupta P. Angiogenic activity of nicotinic acetylcholine receptors: Implications in tobacco-related vascular diseases. Pharmacol. Therapeutics. 2009; 121:205–223.

Erhardt L. Cigarette smoking: an undertreated risk factor for cardiovascular disease. Atherosclerosis. 2009; 205:23–33. [PubMed: 19217623]

Everts V, Korper W, Niehof A, Jansen I, Beertsen W. Type VI collagen is phagocytosed by fibroblasts and digested in the lysosomal apparatus: involvement of collagenase, serine proteinases and lysosomal enzymes. Matrix Biol. 1994; 14:665–676. [PubMed: 9057816]

Eves R, Webb BA, Zhou S, Mak AS. Caldesmon is an integral component of podosomes in smooth muscle cells. J. Cell Sci. 2006; 119:1691–1702. [PubMed: 16595550]

Gimona M, Buccione R. Adhesions that mediate invasion. International J. Biochem. Cell Biol. 2006; 38:1875–1892.

Gu Z, Kordowska J, Williams GL, Wang CLA, Hai CM. Erk1/2 MAPK and caldesmon differentially regulate podosome dynamics in A7r5 vascular smooth muscle cells. Exp. Cell. Res. 2007; 313:849–866. [PubMed: 17239373]

Hai CM, Hahne P, Harrington EO, Gimona M. Conventional protein kinase C mediates phorbol-dibutyrate-induced cytoskeletal remodeling in A7f5 smooth muscle cells. Exp. Cell Res. 2002; 280:64–74. [PubMed: 12372340]

Heeschen C, Jang JJ, Weis M, Pathak A, Kaji S, Hu RS, Tsao PS, Johnson FL, Cooke JP. Nicotine stimulates angiogenesis and promotes tumor growth and atherosclerosis. Nature Med. 2001; 7:833–839. 2001. [PubMed: 11433349]

Jenkins GM, Crow MT, Bilato C, Gluzband Y, Ryu WS, Li Z, Stetler-Stevenson W, Nater C, Froehlich JP, Lakatta EG, Cheng L. Increased expression of membrane-type matrix metalloproteinase and preferential localization of matrix metalloproteinase-2 to the neointima of balloon-injured rat arteries. Circulation. 1998; 97:82–90. [PubMed: 9443435]

Kuzuya M, Nakamura K, Sasaki T, Cheng XW, Itohara S, Iguchi A. Effect of MMP-2 deficiency on atherosclerotic lesion formation in AproE-deficient mice. Arterioscler. Throm. Vasc. Biol. 2006; 26:1120–1125.

Lee SD, Lee DS, Chun YG, Shim TS, Lim CM, Koh Y, Kim WS, Kim DS, Kim WD. Cigarette smoke extract induces endothelin-1 via protein kinase C in pulmonary artery endothelial cells. Am. J. Physiol. Lung Cell Mol. Physiol. 2001; 281:L403–L411. [PubMed: 11435215]

Li S, Zhao T, Xin H, Ye LH, Zhang X, Tanaka H, Nakamura A, Kohama K. Nicotinic acetylcholine receptor α7 subunit mediates migration of vascular smooth muscle cells toward nicotine. J. Pharmacol. Sci. 2004; 94:334–338. [PubMed: 15037820]

Linder S. The matrix corroded: podosomes and invadopodia in extracellular matrix degradation. Trends Cell Biol. 2006; 17:107–117. [PubMed: 17275303]

Madsen DH, Engelholm LH, Ingversen S, Hillig T, Wagenaar-Miller RA, Kjoller L, Gardsvoll H, Hoyer-Hansen G, Holmbeck K, Bugge TH, Behrendt N. Extracellular collagenases and the endocytic receptor, urokinase plasminogen activator receptor-associated protein/Endo180, cooperate in fibroblast-mediated collagen degradation. J. Biol. Chem. 2007; 282:27037–27045. [PubMed: 17623673]

Maqbool A, Keswani A, Galloway S, O'Regan DJ, Ball SG, Turner NA, Porter KE. MMP-3 (5A/6A) polymorphism does not influence human smooth muscle cell invasion. J. Surg. Res. 2012; 175:343–349. [PubMed: 21601886]

Moise L, Zeng H, Caffery P, Rogowski RS, Hawrot E. Structure and function of alpha-bungarotoxin. J. Toxicol. Toxin Rev. 2002; 21:293–317.

Moreyra AE, Lacy CR, Wilson AC, Kumar A, Kostis JB. Arterial blood nicotine concentration and coronary vasoconstrictive effect of low-nicotine cigarette smoking. Am. Heart J. 1992; 124:392–397. [PubMed: 1636583]

Newby AC. Dual role of matrix metalloproteinases (matrixins) in intimal thickening and atherosclerotic plaque rupture. Physiol. Rev. 2005; 85:1–31. [PubMed: 15618476]

Ng MKC, Wu J, Chang E, Wang B-Y, Katzenberg-Clark R, Ishii-Watabe A, Cooke JP. A central role for nicotinic cholinergic regulation of growth factor-induced endothelial cell migration. Arterioscler. Thromb. Vasc. Biol. 2007; 27:106–112. [PubMed: 17082486]

Obejero-Paz CA, Auslender M, Scarpa A. PKC activity modulates availability and long openings of L-type Ca^{2+} channels in A7r5 cells. Am. J. Physiol. 1998; 275:C535–C543. [PubMed: 9688608]

Proszynki TJ, Gingras J, Valdez G, Krzewski K, Sanes JR. Podosomes are present in a postsynaptic apparatus and participate in its maturation. Proc. Natl. Acad. Sci. USA. 2009; 106:18373–18378. [PubMed: 19822767]

Sperti G, Colucci WS. Phorbol ester-stimulated bidirectional transmembrane calcium flux in A7r5 vascular smooth muscle cells. Mol. Pharmacol. 1987; 32:37–42. [PubMed: 2439892]

Su Y, Han W, Giraldo C, De Li Y, Block ER. Effect of cigarette smoke extract on nitric oxide synthase in pulmonary artery endothelial cells. Am. J. Respir. Cell. Mol. Biol. 1998; 19:819–825. [PubMed: 9806747]

Varon C, Tatin F, Moreau V, Van Obberghen-Schilling E, Fernandez-Sauze S, Reuzeau E, Kramer I, Genot E. Transforming growth factor β induces rosettes of podosomes in primary aortic endothelial cells. Mol. Cell. Biol. 2006; 26:3582–3594. [PubMed: 16611998]

Vijayaraghavan S, Pugh PC, Zhang ZW, Rathouz MM, Berg DK. Nicotinic receptors that bind α-bungarotoxin on neurons raise intracellular free Ca2+ Neuron. 1992; 8:353–362. [PubMed: 1310863]

Wang J, Yin G, Menon P, Pang J, Smolock EM, Yan C, Berk BC. Phosphorylation of G protein-coupled receptor kinase 2-interacting protein 1 tyrosine 392 is required for phospholipase C-gamma activation and podosome formation in vascular smooth muscle cells. Arterioscler. Thromb. Vasc. Biol. 2010; 30:1976–1982. [PubMed: 20689073]

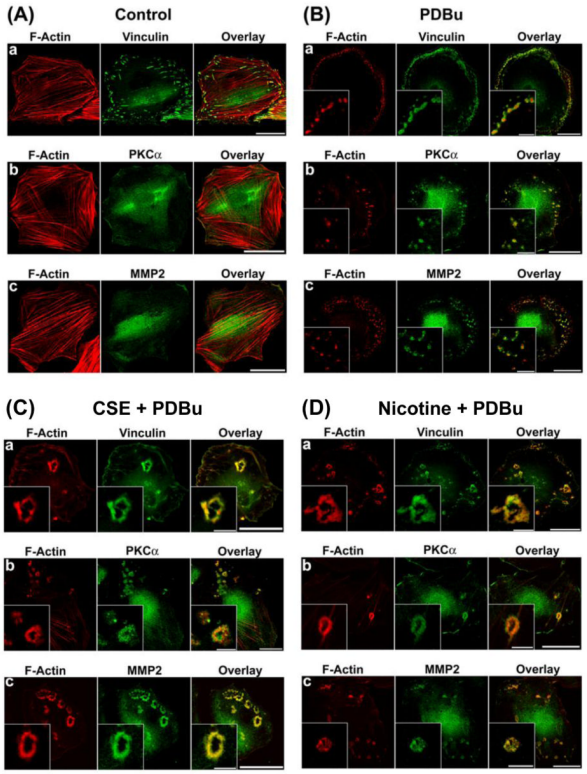

Figure 1.

Cigarette smoke extract (CSE) and nicotine-treated A7r5 cells formed podosome rosettes in response to PKC activation by *phorbol-12,13-dibutyrate (PDBu)*. This figure shows confocal microscopic images of: a) F-actin and vinculin, b) F-actin and PKC-α, and c) F-actin and MMP-2 in: A) unstimulated untreated (control), B) PDBu-stimulated, untreated, C) PDBu-stimulated, CSE-treated, and D) PDBu-stimulated, nicotine-treated A7r5 cells. CSE treatment consisted of treating cells with 5% CSE for 6 hr prior to stimulation by 1 μM PDBu for 1 hr. Nicotine treatment consisted of treating cells with 2 μM nicotine for 6 hr prior to stimulation by 1 μM PDBu for 1 hr. F-actin was labeled in red. Vinculin, PKC-α, and MMP-2 were labeled in green. Insets in panels B and D represent higher magnification of selected regions of the cell to show the structure of podosomes and podosome rosettes. Horizontal bars in main panels represent 40 μm, whereas horizontal bars in insets represent 8 μm.

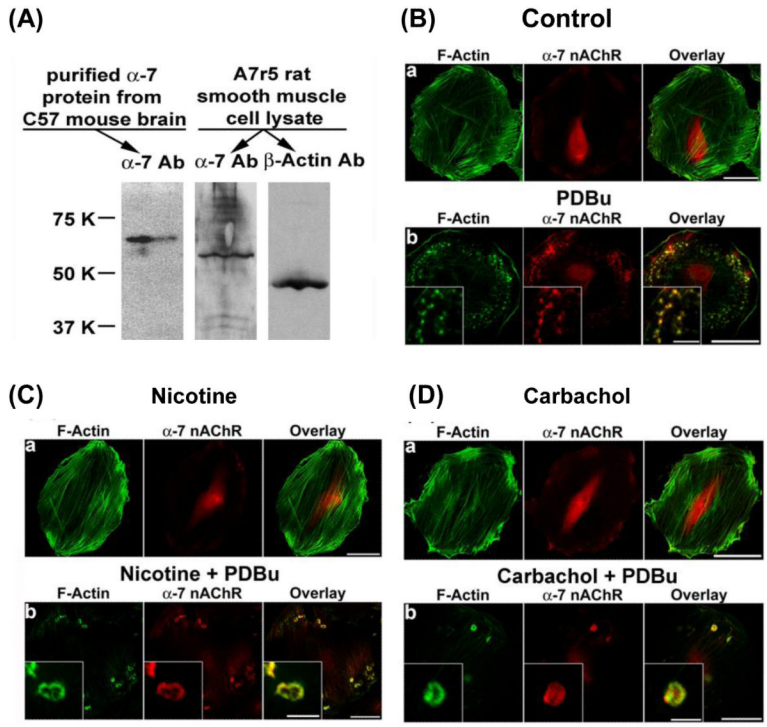

Figure 2.

Localization of α7-nicotinic acetylcholine receptors in A7r5 cells as demonstrated by Western blotting and immunofluorescence microscopy. Panel A shows immunoblots of α7-nicotinic acetylcholine receptor in C57 mouse brain extract (left lane; positive control), and α7-nicotinic acetylcholine receptor (center lane) and β-actin (right lane) in A7r5 cell lysate. Panels B-D show confocal microscopic images of α7-nicotinic acetylcholine receptor and F-actin in unstimulated and PDBu-stimulated A7r5 cells. Nicotine and carbachol treatment consisted of treating cells with 2 μM nicotine hydrogen tartrate or carbachol for 6 hr prior to stimulation by 1 μM PDBu for 1 hr. F-actin was labeled in green. α7-Nicotinic acetylcholine receptor was labeled in red. Insets in panels B, C, and D represent higher magnification of selected regions of the cell to show the structure of podosomes and podosome rosettes. Horizontal bars in main panels represent 40 μm, whereas horizontal bars in insets represent 8 μm.

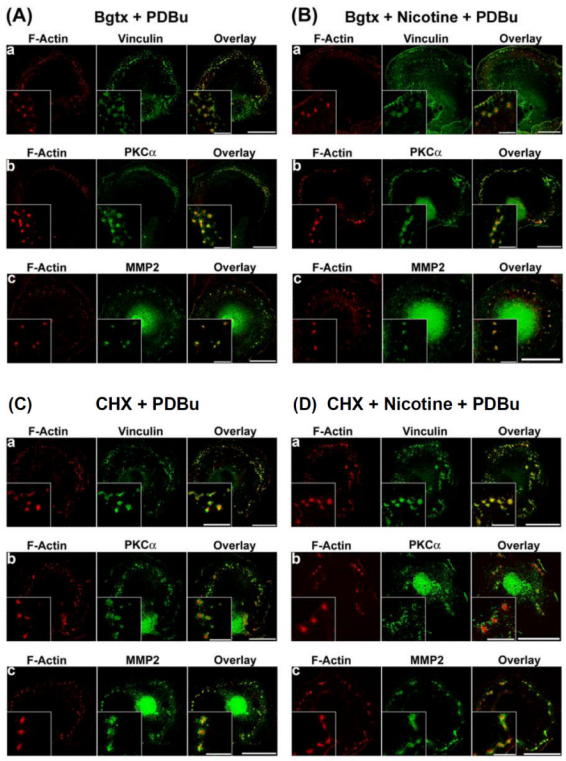

Figure 3.

Effects of α-bungarotoxin (Bgtx) and cycloheximide (CHX) on nicotine-induced cytoskeletal remodeling in A7r5 cells. In α-bungarotoxin experiments (Panels A and B), cells were treated with 0.5 μM α-bungarotoxin or (0.5 μM α-bungarotoxin + 2 μM nicotine) for 6 hr before stimulation by 1 μM PDBu for 1 hr. In cycloheximide experiments (Panels C and D), cells were treated with cycloheximide (50 μg/ml) or (cycloheximide (50 μg/ml) + 2 μM nicotine) for 6 hr before stimulation by 1 μM PDBu for 1 hr. F-actin was labeled in red. Vinculin, PKC-α, and MMP-2 were labeled in green. Insets represent higher magnification of selected regions of the cell to show the structure of podosomes or podosome rosettes. Horizontal bars in main panels represent 40 μm, whereas horizontal bars in insets represent 8 μm.

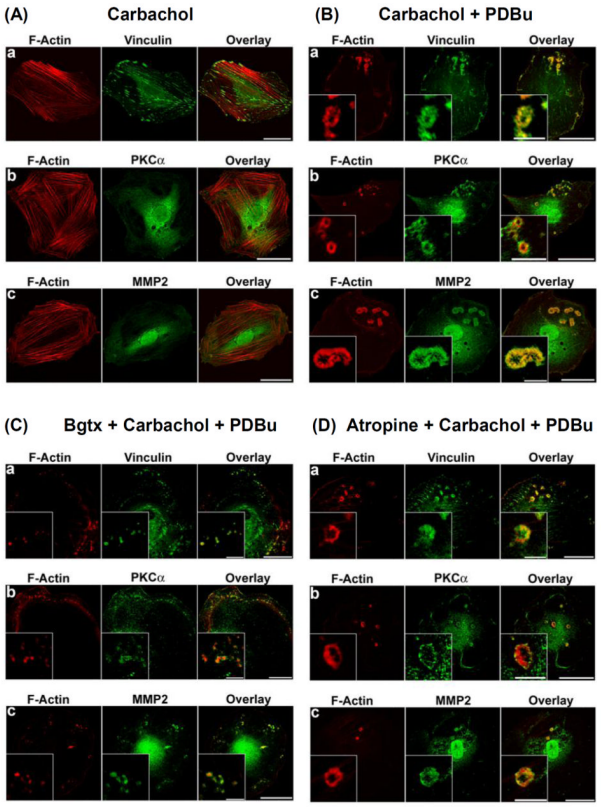

Figure 4.

Effects of α-bungarotoxin (Bgtx) and atropine on carbachol-stimulated cytoskeletal remodeling in A7r5 cells. Panels A and B show confocal microscopic images of: a) F-actin and vinculin, b) F-actin and PKC-α, and c) F-actin and MMP-2 in: A) unstimulated carbachol-treated, and B) PDBu-stimulated, carbachol-treated A7r5 cells. Carbachol treatment consisted of treating cells with 2 μM carbachol for 6 hr before stimulation by 1 μM PDBu for 1 hr. F-actin was labeled in red by Alexa Fluor 568-conjugated phalloidin. Vinculin, PKC-α, and MMP-2 were labeled in green by specific primary antibodies, followed by Alexa Fluor 488-conjugated secondary antibody. Insets in panel B represent higher magnification of selected regions of the cell to show the structure of podosome rosettes. Horizontal bars in main panels represent 40 μm, whereas horizontal bars in insets represent 8 μm. Panels C and D show the effects of α-bungarotoxin and atropine on the formation of podosomes and podosome rosettes in A7r5 cells. In α-bungarotoxin experiments (panel C), cells were treated with 0.5 μM α-bungarotoxin for 1 hr, and then treated with (0.5 μM α-bungarotoxin + 2 μM carbachol) for 6 hr before stimulation by 1 μM PDBu for 1 hr. In atropine experiments (panel D), cells were treated with 2 μM atropine for 1 hr, and then treated with (1 μM atropine + 2 μM carbachol) for 6 hr before stimulation by 1 μM PDBu for 1 hr. F-actin was labeled in red by Alexa Fluor 568-conjugated phalloidin. Vinculin, PKC-α, and MMP-2 were labeled in green by specific primary antibodies, followed by Alexa Fluor 488-conjugated secondary antibody. Insets represent higher magnification of selected regions of the cell to show the structure of podosomes or podosome rosettes. Horizontal bars in main panels represent 40 μm, whereas horizontal bars in insets represent 8 μm.

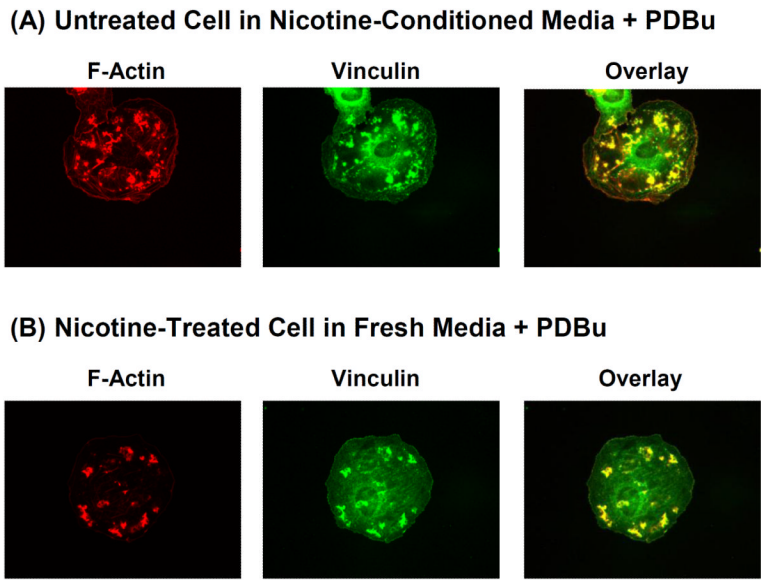

Figure 5.

PDBu-stimulated cytoskeletal remodeling of: (A) untreated A7r5 cells placed in conditioned media collected from culture of nicotine-treated A7r5 cells, and (B) extensively washed nicotine-treated A7r5 cells in fresh media. In panel A, donor A7r5 cells were treated with 2 μM nicotine for 6 hr to produce the conditioned media, which was collected to treat recipient A7r5 cells for 1 hr, followed by 1 μM PDBu stimulation for 1 hr. In panel B, A7r5 cells were treated with 2 μM nicotine for 6 hr, washed in fresh media 5 times, incubated in fresh media for 1 hr, and then stimulated with 1 μM PDBu for 1 hr. F-actin was labeled in red. Vinculin was labeled in green.

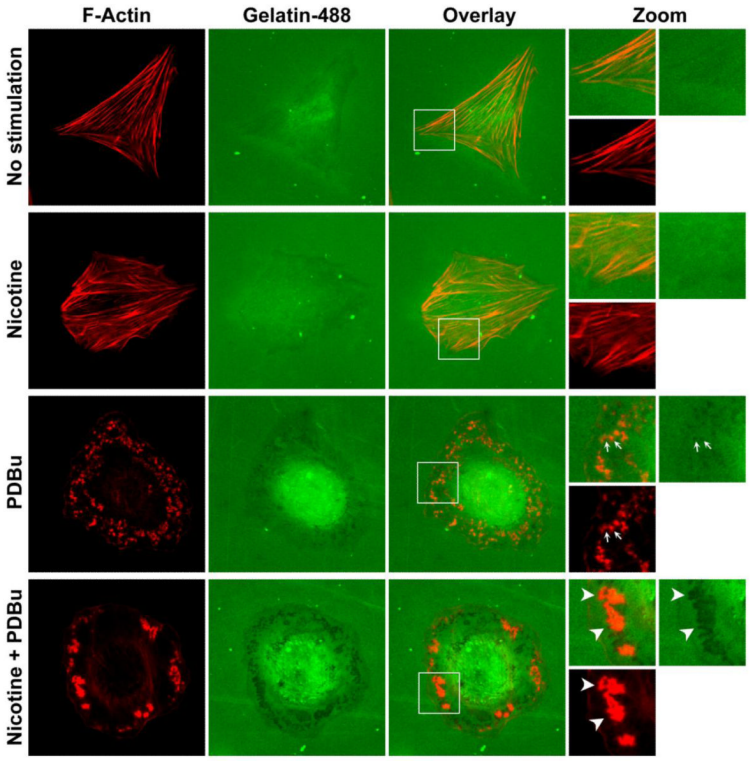

Figure 6.

In situ zymography of cross-linked Alexa Fluor 488-conjugated gelatin degradation by: untreated, unstimulated (top row), nicotine-treated, unstimulated (second row), untreated, PDBu-stimulated (third row), and nicotine-treated, PDBu-stimulated (fourth row) A7r5 cells. F-actin was labeled in red. Alexa Fluor 488-conjugated gelatin is labeled in green. Selected regions of cells were magnified ("Zoom") with the addition of arrows to show degradation of Alexa Fluor 488-conjugated gelatin in the proximity of podosomes and podosome rosettes.

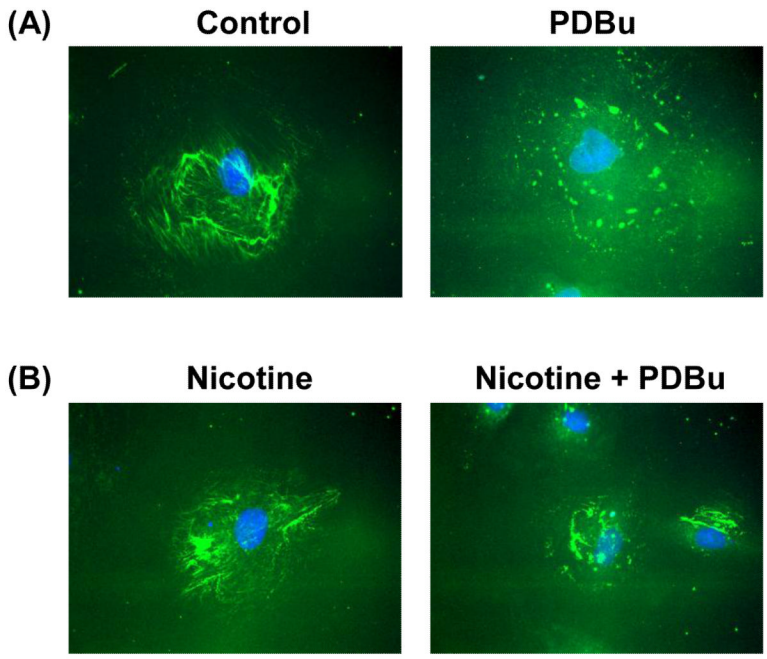

Figure 7.
In situ zymography of DQ-gelatin degradation by: (A) untreated control, and (B) nicotine-treated A7r5 cells before (left panels) and after (right panels) PDBu stimulation. Green fluorescence indicates degradation product of DQ-gelatin. Blue fluorescence indicates DAPI-labeling of nucleus.

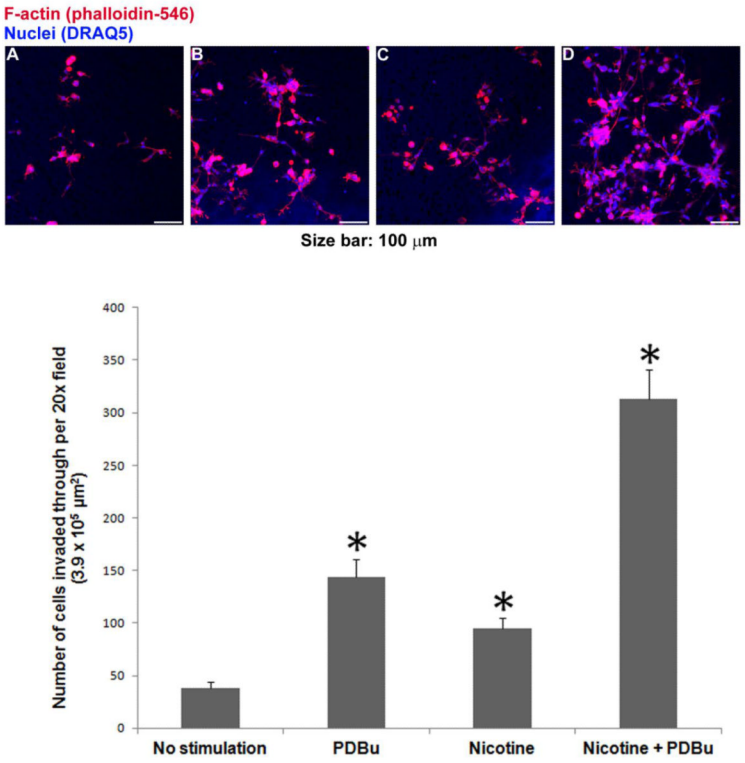

Figure 8.

Nicotine and PDBu-induced invasion of human aortic smooth muscle cells through extracellular matrix, as measured by matrigel-coated transwell invasion assay. Top panels A to D show representative images of cells reaching the bottom side of the membrane under the following four experimental conditions: (A) No Stimulation: neither nicotine nor PDBu was added to the top or bottom chamber; (B) PDBu: 2 μM PDBu in the bottom chamber only; (C) Nicotine: 2 μM nicotine in both top and bottom chambers; and (D) Nicotine + PDBu: 2 μM nicotine in top chamber; 2 μM nicotine and 2 μM PDBu in the bottom chamber. Fluorescence from DRAQ5-labeled nuclei appeared as blue, whereas Alexa Fluor 546-conjugated phalloidin-labeled filamentous actin appeared as red. For each membrane, the number of cells in the 20x microscopic field was counted based on DRAQ5-labeled nuclei. Bottom graph shows cell counts in mean + one standard deviation (n = 3). Asterisks indicate significant difference from control (no stimulation). In addition, two-way ANOVA was performed to analyze individual and interactive effects of PDBu and nicotine on cell invasion.